

each other. In their computational study, Zang et al.³ also captured the interaction between opposing shear layers, but they infer that the incipient hairpin vortex in the lower half of the channel is "swallowed" by the counter-rotating vorticity due to the shear layer in the upper half. In the present calculations we do not observe this swallowing effect. As evident from the vortex line plots, our results point toward the full development of the lambda vortex and the hairpin vortex. Finally, Fig. 4 presents streamwise vorticity contours at fixed x_1 locations corresponding to the tip of the hairpin and displays the evolution of this vortical structure already depicted from the vortex-line plots and the velocity vectors. At later times, the streamwise vorticity contours reveal the development of several pairs of counter-rotating vortices instigated from the breakdown of the primary vortex.

Concluding Remarks

In this work, channel flow transition is visualized through the use of vortex lines representing vortex sheets. These vortex lines track the evolution of nonlinear structures, which manifest themselves as vortex tubes and hairpin vortices.

References

- ¹Williams, D. R., "Vortical Structures in Breakdown Stage of Transition," *ICASE/NASA Workshop on Stability of Time-Dependent and Spatially Varying Flows*, D. L. Dwoyee and M. Y. Hussaini, eds., Springer-Verlag, New York, 1985.
- ²Biringen, S., "Three-Dimensional Structures of Transition in Plane Channel Flows," *Physics of Fluids*, Vol. 30, Nov. 1987, pp. 3359-3368.
- ³Zang, T. A., Krist, S. E., Erlebacher, G., and Hussaini, M. Y., "Nonlinear Structures in the Later Stages of Transition," *AIAA Paper 87-1024*, 1987.
- ⁴Gilbert, N. and Kleiser, L., "Near-Wall Phenomena in Transition to Turbulence," Zoran Zaric International Seminar on Near-Wall Turbulence, Dubrovnik, Yugoslavia, May 16-20, 1988.
- ⁵Biringen, S., "Final Stages of Transition to Turbulence in Plane Channel Flow," *Journal of Fluid Mechanics*, Vol. 148, Nov. 1984, pp. 413-442.
- ⁶Head, M. R. and Bandyopadhyay, P., "New Aspects of Turbulent Boundary-Layer Structure," *Journal of Fluid Mechanics*, Vol. 107, June 1981, pp. 297-338.
- ⁷Moin, P., Leonard, A., and Kim, J., "Evolution of a Curved Vortex Filament Into a Vortex Ring," *Physics of Fluids*, Vol. 29, April 1986, pp. 955-963.
- ⁸Krist, S. E. and Zang, T. A., "Numerical Simulation of Channel Flow Transition," *NASA TP-2667*, April 1987.

Acknowledgment

This work was performed under Grant NAG-1-798 from NASA Langley Research Center.

Control of Natural Laminar Instability Waves on an Axisymmetric Body

Daniel M. Ladd*

Naval Ocean Systems Center
San Diego, California

Introduction

THE response of a two-dimensional laminar boundary-layer instability (so called Tollmien-Schlichting, or TS, waves) to wave superposition has been the subject of several

recent investigations. Liepmann et al.¹ demonstrated the generation of artificial TS waves on a flat plate using periodic pulsing of heaters embedded in a flat plate in water. Later, Liepmann and Nosenchuck² used this technique to actively attenuate the "naturally" occurring TS waves and to increase the length of laminar flow on the flat plate. Gedney³ used plate vibration to attenuate sound-produced artificial TS waves. Thomas⁴ used two vibrating ribbons on a flat plate in air. Milling⁵ performed a similar operation with vibrating ribbons in a water channel. Except for Liepmann and Nosenchuck,² all of these experiments used artificially produced TS waves. The logical progression of this technique is the ability to deal with random disturbances, as would be found in most flows of interest. This experiment addresses that problem.

Experimental Apparatus

The facility used was the Naval Ocean Systems Center high-speed water tunnel. This tunnel has a 305-mm circular open jet, where velocities up to 15 m/s are possible. The turbulence level (u'/U_∞) is a respectable 0.16% throughout the speed range.

The axisymmetric body used was a 9:1 fineness ratio ellipsoid of revolution. The diameter of the midsection was 50 mm. The ellipsoid maintained a true elliptical outline until an axial distance (x) of 397 mm, at which point constant slope was maintained to intercept the support diameter of 25.4 mm. The pressure distribution of this model is similar to a Reichardt body and is very flat, making this model essentially the axisymmetric equivalent of a flat plate. Previous experiments with identically shaped models have shown transition Reynolds numbers of about 2.8 million, which agrees well with the measured 0.16% turbulence level of the tunnel.

It was found that the "natural" TS waves occurring on this body would form wave packets, whose phase and amplitude were random. For the case presented here, the frequencies of the wave packets ranged from approximately 700 to 1400 Hz. The origin of these waves was presumably from the background freestream turbulence of the tunnel (hence the term "natural" as opposed to artificially produced). Comparison with spatial linear stability theory showed the center of the TS wave frequency spectrum to follow the upper branch of the linear stability curve. This is expected behavior for a body with a flat pressure distribution, whose stability curve is essentially unchanged with axial location. At frequencies higher than the center frequency, the TS waves are being damped, eventually to be of no concern. Frequencies lower than center are still in the process of being amplified, yet to reach overall peak amplification. The center frequency has reached its peak amplification and is about ready to be damped (e.g., zero amplification rate, the upper branch of the stability curve).

Method and Results

The control of randomly occurring TS waves requires a sensor before or coincident with the control actuator. Here the sensors are flush-mounted hot films. This model had the control actuator at a location well downstream from the nose. This allowed an ambient TS wave to amplify enough such that a shear-stress sensor could reasonably be expected to sense the presence of a TS wave before arriving at the actuator. This requires an actuator that can produce large control perturbations.

Our goal for an actuator design was to be able to produce a perturbation of 1% of freestream velocity at a frequency of 1000 Hz. Initial attempts at using a strip heating element as in Ref. 6 failed to produce a survivable heater element that could produce the required perturbation. A different design was tried that used a small commercially available acoustic speaker with a 21.6-mm stainless-steel diaphragm. This speaker fit conveniently inside the model, with the diaphragm perpendicular to the model axis. The function of the speaker diaphragm was to change the volume of a small cavity inside the model, to produce suction/blowing through a circumferential slot, oriented normal to the flow. The slot wide was about

Received Dec. 15, 1988; presented as Paper 89-0037 at the 27th Aerospace Sciences Meeting, Reno, NV, Jan. 8-12, 1989; revision received May 26, 1989. This paper is declared a work of the U.S. Government and is not subject to copyright protection in the United States.

*Hydrodynamicist. Member AIAA.

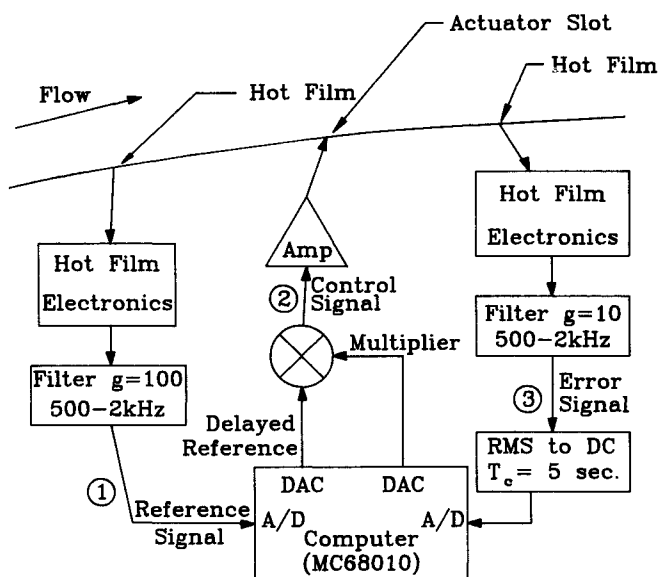


Fig. 1 Block diagram for "invert-and-delay" control loop. Numbers correspond to traces in Figs. 2 and 3.

0.075 mm and was essentially continuous around the model. The axial location of the suction/blowing slot was 130 mm. Also installed was a flush-mounted hot-film sensor at an axial location of 125 mm (just before the slot) and another sensor directly downstream at an axial location of 152 mm. It was found that this actuator was very capable of producing large shear perturbations on the downstream hot-film sensor. Although the slot would produce a suction/blowing perturbation around the circumference of the model, this experiment could deal only with one azimuthal location (the top or 0 deg). No attempt was made to address the problem of the circumferential variation of the TS waves on this body (which were considerable and seemed to be related to the low-frequency background turbulence).

An extremely simple (minded) control system was devised for this system (Fig. 1). The control signal applied to the actuator slot was a time-delayed image of the signal arriving at the forward shear sensor (labeled "reference signal"). The gain (multiplying factor) and time delay are initially unknown, being various functions of TS wave growth, phase speed, mechanical phase lag, filter delay, power amplifier gain, etc. The function of the controller is to adjust the variables of time delay and gain factor such that a minimum signal (rms) appears at the downstream hot film. A hybrid digital-to-analog controller system was developed to perform these functions. The digital portion of the system implemented the time-delay loop and the binary search algorithm for the time delay and gain. The functions of gain multiplying and rms calculation were performed using analog circuit elements. The simple optimization algorithm used an initial guess for time delay and the initial gain and time-delay increments. A binary search was then performed for the optimum time delay and gain. The search increments were normalized to the rms voltage of the second sensor (i.e., smaller rms, smaller step sizes). This type of control system has been called an "invert-and-delay" type of control.

Figures 2 and 3 show the action of this control system on TS waves at a freestream velocity of 8.67 m/s. Figure 2 is the forward and aft shear-stress signals with no control. Figure 3 is the same conditions after control. For the particular sample records shown, the ratio of the aft shear-stress rms to the fore shear stress has been reduced by about 55% with control. Using a 5-s running average, the rms voltage has been reduced by about 53% after control.

Conclusions

Figure 3 shows that random Tollmien-Schlichting waves can be controlled, to some extent, using a suction/blowing slot

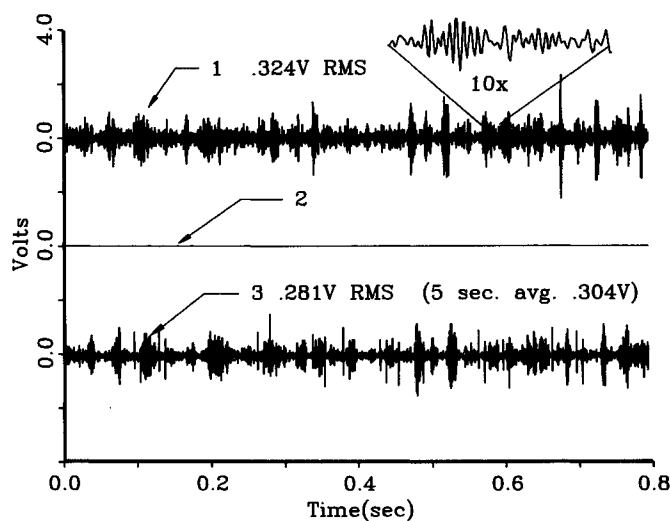


Fig. 2 Tollmien-Schlichting waves, no control: $U_\infty = 8.67$ m/s, $T_\infty = 24.1^\circ\text{C}$. Trace 1—hot-film voltage: $x = 123.8$ mm; gain = 100x; filtered 500 Hz–2 kHz; $Re_\delta = 1479$. Trace 2—control voltage. Trace 3—hot-film voltage: $x = 151.6$ mm; gain = 10x; $Re_\delta = 1658$.

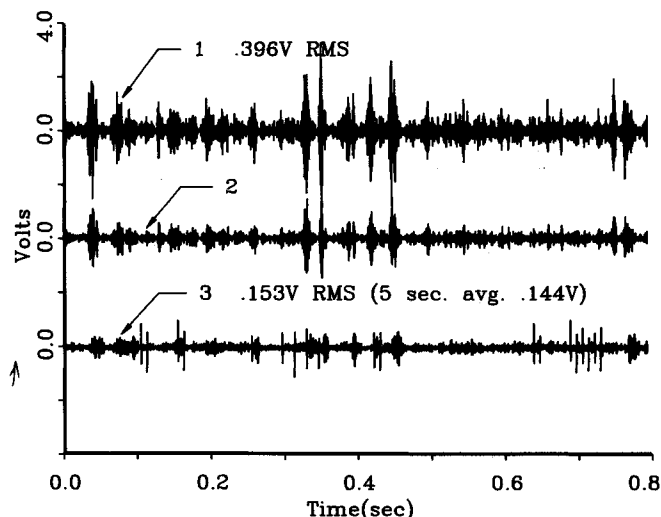


Fig. 3 Tollmien-Schlichting waves with control; same conditions as in Fig. 2.

and a simple control algorithm. The suction/blowing slot appears to be a powerful method of introducing perturbations into a laminar boundary layer. The implementation of the invert-and-delay algorithm used in the present study is in no way optimum, but was only a first attempt at control. In this experiment, the transfer function from the forward hot-film sensor to the suction/blowing slot is approximated with a single time delay and gain. A more sophisticated control loop would include the effects of TS wave frequency on phase speed and amplification and, presumably, would achieve better control.

Acknowledgments

This investigation was originally supported under the Naval Ocean Systems Center Internal Research Program and later by the Office of Naval Research.

References

- Liepmann, H. W., Brown, G. L., and Nosenchuck, D. M., "Control of Laminar-Instability Waves Using a New Technique," *Journal of Fluid Mechanics*, Vol. 118, May 1982, pp. 187–200.
- Liepmann, H. W. and Nosenchuck, D. M., "Active Control of Laminar-Turbulent Transition," *Journal of Fluid Mechanics*, Vol. 118, May 1982, pp. 201–204.

³Gedney, C. J., "The Response of a Laminar Boundary Layer to Sound and Wall Vibration," Massachusetts Institute of Technology, Cambridge, MA, Rept. 83560-3, May 1983.

⁴Thomas, A. S. W., "The Control of Boundary Layer Transition Using a Wave-Superposition Principle," *Journal of Fluid Mechanics*, Vol. 137, Dec. 1983, pp. 233-250.

⁵Milling, R. W., "Tollmien-Schlichting Wave Cancellation," *Physics of Fluids*, Vol. 24, May 1981, pp. 979-981.

⁶Ladd, D. M. and Hendricks, E. W., "Active Control of 2-D Instability Waves on an Axisymmetric Body," *Experiments in Fluids*, Vol. 6, No. 1 1988, pp. 69-70.

Analytical Modeling of Nonradial Expansion Plumes

Iain D. Boyd*

University of Southampton, Southampton, England,
United Kingdom

Introduction

THE Simons model^{1,2} is a simple analytical model used in the calculation of axisymmetric rocket and thruster exhaust plume flowfields. The model proposes that the density ρ at the point (r, θ) in the axisymmetric plane is given by

$$\rho(r, \theta) = \frac{A}{r^2} f(\theta) \quad (1)$$

where A is the plume constant and $f(\theta)$ is the angular density distribution. It is therefore assumed that the density diverges radially. A description of the procedures for the determination of A and $f(\theta)$ for a particular nozzle geometry and gas type are included in Ref. 2.

Due to its analytical nature, the Simons model is a widely used engineering tool. It is often employed, for example, in the swift calculation of impingement effects associated with a satellite attitude control thruster system.³

It has been shown by Boyd and Stark⁴ that, for certain plumes of nitrogen expanding from small nozzles, the assumption of radial decay gives rise to unsatisfactory results in calculations made with the Simons model. Errors of up to 50% were noted for the prediction of the density distribution along the plume axis for which experimental data was available. This phenomenon was observed to occur for nozzles having a large exit Mach number and/or a large nozzle exit half-angle. By making successful method of characteristics calculations of similar plumes, a new analytical formulation was derived. This new method has been termed the Modified Simons model and allows the nonradial nature of such plumes to be successfully predicted. Specifically, the assumption of radial expansion is replaced in the Modified Simons model by the following:

$$\rho(r, \theta) = \frac{A}{r^2 - ar + b} f(\theta) \quad (2)$$

where

$$a = 3\theta_E^{1/2} Ma_E r_E \quad (3a)$$

$$b = 5\theta_E Ma_E^2 r_E^2 \quad (3b)$$

In Eqs. (3), θ_E is the nozzle exit half-angle expressed in radians, Ma_E the nozzle exit Mach number, and r_E the nozzle exit radius. The exit Mach number is obtained by iterative solution of the following expression for the ratio of the area at the

nozzle exit to that at the nozzle throat:

$$\epsilon = \frac{1}{Ma_E} \sqrt{\left[\frac{1 + \frac{\gamma-1}{2} Ma_E^2}{1 + \frac{\gamma-1}{2}} \right]^{\frac{\gamma+1}{\gamma-1}}} \quad (4)$$

where γ is the ratio of specific heats. The area at the nozzle exit is that reduced by the presence of any boundary-layer thickness along the nozzle wall. Under certain conditions it is possible for the denominator in Eq. (2) to become negative. Generally, the behavior of the model at distances of less than 5 exit radii from the nozzle is not reliable.

While these expressions have been derived for the expansion of nitrogen, which has $\gamma = 1.4$, it was shown in Ref. 4 that their application to a hydrazine plume, in which $\gamma = 1.37$, also gave significant improvement on the original Simons model when compared with experimental data. The expressions have therefore been found to be of great value in improving the prediction of plume flows for gases in which the ratio of specific heats is close to that for a diatomic gas.

For most expansion plume investigations undertaken in the laboratory, the test gas is nitrogen. But in real propulsion applications the use of solid fuel and bipropellant systems is more common. Depending on the specific fuels employed, the ratio of specific heats may be very different from 1.4. It is therefore the purpose of the present study to determine the usefulness of the Modified Simons model as applied to monatomic and polyatomic gas expansions.

Calculations

The expansion of nitrogen (N_2), argon (Ar), and tetrafluoromethane (CF_4) through a number of nozzles has been investigated experimentally by Legge et al.⁵ One of the nozzles considered is the MBB/ERNO 0.5N thruster. This engine is designed to burn monopropellant hydrazine and its expansion plume has received detailed analysis by Boyd and Stark.⁶ In the present study, calculation is made of the expansion of the three test gases through this nozzle and the results are compared with experimental data obtained along the plume axis.⁷

Although the nozzle geometry is fixed, the structure of the exhaust plumes for the three different gases is quite different. In addition to having different values for γ (see Table 1), viscosity effects along the nozzle wall will also be important. For the small dimensions of this thruster (the exit radius is less than 3 mm), a thick laminar boundary layer exists at the nozzle exit plane. The reduction in volume of the inviscid flow at the nozzle exit plane reduces the exit Mach number as calculated by Eq. (4), and thus has a direct effect on Eqs. (3). It is this aspect of such calculations that makes difficult the derivation of a more generalized Modified Simons model. The calculated exit plane quantities, together with the plume constant employed, are listed in Table 1 for each of the gases.

In Fig. 1 the distribution of Pitot pressure along the plume axis is shown for the expansion of nitrogen. The improvement provided by the Modified Simons model is quite apparent. Calculations made with the original Simons model are found to be in error by as much as 35% when compared with the experimental data obtained in the near field of the plume. Although the two sets of theoretical solutions are observed to converge at larger distances along the axis, there is still an error of 11% associated with the original Simons model result obtained at the last available experimental data point. The corresponding value obtained with the Simons model shows a deviation of just 3% from the experiment.

The expansion of monatomic argon is now considered. The ratio of the theoretical predictions of pitot pressure to the values obtained experimentally are plotted in Fig. 2. The improvement attained with the Modified model in comparison to the results obtained with the original Simons model are quite satisfying. A significant improvement in the results is found particularly at larger distances from the nozzle exit plane. Similar plots for tetrafluoromethane are shown in Fig. 3. Once

Received Oct. 24, 1988; revision received March 13, 1989. Copyright © 1989 American Institute of Aeronautics and Astronautics, Inc. All rights reserved.

*Graduate Student, Department of Aeronautics and Astronautics; currently, Research Scientist, NASA Ames Research Center, Moffett Field, CA.